



Short communication

Photo-excitation enhanced high temperature conductivity and crystallization kinetics in ultra-thin $\text{La}_{0.6}\text{Sr}_{0.4}\text{Co}_{0.8}\text{Fe}_{0.2}\text{O}_{3-\delta}$ filmsTyler Cain¹, Bo-Kuai Lai, Subramanian Sankaranarayanan, Shriram Ramanathan*

School of Engineering and Applied Sciences, Harvard University, Cambridge, MA 02138, United States

ARTICLE INFO

Article history:

Received 13 November 2009

Accepted 21 November 2009

Available online 2 December 2009

Keywords:

Lanthanum strontium cobalt ferrite

Solid oxide fuel cell

Cathode

Ultra-thin film

Nanocrystalline

Photo-excitation

ABSTRACT

The synthesis of high performance nanostructured oxide electrodes is critical to advancement of energy technologies such as intermediate temperature solid oxide fuel cells. In this communication, we demonstrate that photo-excitation during crystallization of nanostructured 60-nm-thick $\text{La}_{0.6}\text{Sr}_{0.4}\text{Co}_{0.8}\text{Fe}_{0.2}\text{O}_{3-\delta}$ films leads to a significant improvement in electrical conductivity. Crystallization kinetics is also enhanced by photo-excitation while the crystallization onset temperature remains similar.

© 2009 Elsevier B.V. All rights reserved.

1. Introduction

Solid oxide fuel cells (SOFCs) have drawn attention for electrical power generation because of their low emissions, high efficiency, and flexibility in fuel sources [1]. SOFCs typically operate at temperatures above 700 °C, creating issues with thermal stress, material selection, and device packaging [2,3]. Efforts are being pursued to operate SOFCs below 600 °C by utilizing thin film structures to reduce many of the impacts of the aforementioned factors [4]. However, reduced operating temperature may also decrease the ionic/electronic conductivity and decrease oxygen reduction reaction rate at the cathodes, due to the thermally activated nature of these processes [5]. To address these issues, it is critical to advance synthesis routes for high performance cathodes with superior electrical conductivity [6,7]. $\text{La}_x\text{Sr}_{1-x}\text{Co}_y\text{Fe}_{1-y}\text{O}_{3-\delta}$ (LSCF) has been explored as a promising cathode material for use in SOFCs [8]. LSCF exhibits mixed ionic and electronic conductivity and high electrocatalytic activity with regards to the oxygen reduction reaction [9]. Recent reports have indicated that LSCF ultra-thin films may be able to perform comparably to thick, porous cathodes [10,11]. Typical

synthesis methods for LSCF require high temperatures, potentially leading to interfacial reactions with the electrolyte [12]. LSCF synthesized by sputtering has been shown to produce functional films that crystallize at ~450 °C and do not react with yttria-stabilized zirconia [9,13–15].

Athermal photo-excitation has been utilized to enhance oxidation rates, increase oxygen incorporation, and influence crystallinity in oxides [16–18]. The interaction of ultraviolet (UV) photons with oxygen can produce oxygen radicals or ozone, dramatically increasing oxygen reactivity on surfaces and enhancing oxygen incorporation into thin films even as low as room temperature (RT) [19]. Changes in electrical and optical properties, as well as lattice parameters, have been observed in perovskite oxide films treated by UV photons [17].

In this paper, we present for the first time results on the effect of UV photo-excitation during crystallization and resulting high temperature conductivity of sputtered $\text{La}_{0.6}\text{Sr}_{0.4}\text{Co}_{0.8}\text{Fe}_{0.2}\text{O}_{3-\delta}$ thin films. *In situ* measurements of in-plane electrical conductivity in a custom designed high temperature probe station were performed during annealing under photo-excitation to observe both the kinetics and onset of LSCF crystallization. The results indicate that UV assisted crystallization can effectively improve structural properties and enhance electrical conductivity of LSCF thin films at relatively low temperatures and the effect is preserved at temperatures up to 550 °C. Since a such treatment method can be performed effectively at temperatures below 550 °C, it could alleviate the aforementioned high temperature-related issues and, thus, is of practical implication for intermediate temperature SOFCs.

* Corresponding author: School of Engineering and Applied Sciences, Harvard University, 29 Oxford St., Pierce Hall, Cambridge, MA 02138, United States. Tel.: +1 617 496 0358; fax: +1 617 497 4627.

E-mail address: shriram@seas.harvard.edu (S. Ramanathan).

¹ Present address: Department of Materials Science and Engineering, University of Illinois at Urbana-Champaign, Urbana, IL 61801, United States.

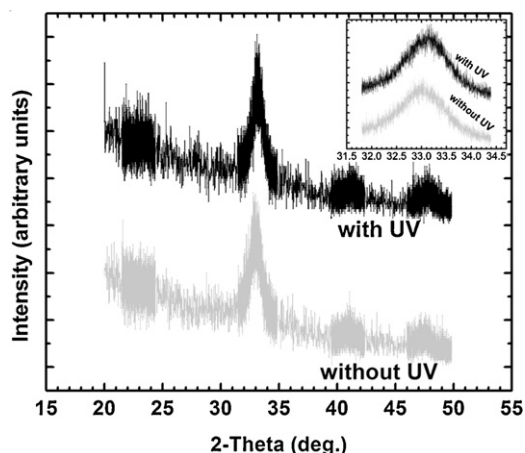


Fig. 1. XRD patterns of 60-nm-thick LSCF films annealed at 450 °C with and without UV irradiation; (inset) XRD peaks near 33° 2 θ .

2. Experimental procedure

$\text{La}_{0.6}\text{Sr}_{0.4}\text{Co}_{0.8}\text{Fe}_{0.2}\text{O}_{3-\delta}$ thin films were RF-sputtered from a stoichiometric target (AJA International) onto single crystalline 8% yttria-stabilized zirconia (YSZ) substrates, measured 10 mm \times 10 mm \times 0.5 mm. Sputtering was carried out at a power of 60 W and at Ar plasma of 5 mTorr, starting from a base pressure of 3×10^{-8} Torr. *In situ* high temperature conductivity studies were performed on 60-nm-thick LSCF films in air with two 210-nm-thick Pt electrodes. The electrodes, measured 9 mm \times 3.1 mm and separated by 2.8 mm, are sputtered on the opposite side of the LSCF-coated substrates using shadow masks. Photon sources built into the probe station enable *in situ* exposure while heating, as well as electrical conductivity measurements. The lamp was separated from the sample surface by 15 mm. The temperature was continuously monitored using type-K thermocouples. Oxygen partial pressure is ~ 0.21 atm for both conductivity measurement and annealing. Note that gentle UV illumination does not lead to any additional sample heating and conductivity values in LSCF do not change when it is turned off, indicating negligible contributions from electronic excitations. X-ray diffraction (XRD) was carried out using Cu K α radiation at an incident angle of 1°. Prior to which, rocking curve measurements were performed to ensure accurate alignment between detector and X-ray tube. Scan steps were set at $0.00125^\circ \text{ s}^{-1}$ for LSCF peaks and at $0.02^\circ \text{ s}^{-1}$ otherwise. Surface morphology was examined by Asylum MFP-3D atomic force microscopy (AFM).

3. Results and discussion

60-nm-thick LSCF films annealed at 450 °C for 2 h with and without UV exposure were studied initially to investigate their crystallinity with XRD. The thin films were grown concurrently. Fig. 1 indicates that both films are crystalline after annealing to 450 °C. XRD peaks around 33°, 41°, and 47° 2 θ correspond to the LSCF (1 1 0)(1 0 4), (2 0 2), and (0 2 4) peaks, respectively [9]. No additional peaks are observed, indicating absence of interfacial reaction between LSCF and YSZ. As seen in the inset of Fig. 1, the position of the $\sim 33^\circ$ peak is 0.1° higher for the film crystallized under UV irradiation compared to the film annealed without UV, indicating a slight decrease in the average lattice parameter of the LSCF thin film. Enhanced oxygen incorporation during annealing could possibly decrease the overall oxygen deficiency in the film, reducing the number of oxygen vacancies [19–21]. Oxygen vacancies may reduce the Coulomb attraction between cations and anions in the lattice, effectively increasing lattice parameter. Such phenomena has been reported for microcrystalline LSCF [8] and similar results have been observed during photon-assisted annealing of (Ba,Sr)TiO $_3$ films [17]. Figs. 2(a) and (b) show AFM images of the LSCF films annealed at 450 °C with and without UV irradiation, respectively. RMS surface roughness measurements for both films are almost identical, nearly 0.5 nm. Note that LSCF and YSZ thin films deposited in a vacuum environment possess a high level of oxygen vacancies and oxygen uptake would occur during heating [9,13,15]. After annealing above 450 °C, oxygen content in the thin films can be stabilized [9,15].

In situ conductivity studies prior to and during onset of crystallization were performed on the LSCF thin films, deposited concurrently, utilizing Pt electrodes. Fig. 3(a) depicts the experimental apparatus used for (simultaneous) high temperature annealing, photon illumination, and electrical measurements. The temperature ramp rate was $10^\circ \text{ C s}^{-1}$ below 350 °C, above which the rate was 2° C s^{-1} up to 450 °C. Temperature was held at 450 °C for ~ 45 min to observe LSCF conductivity changes with annealing time. Annealing temperature was subsequently increased to 550 °C and held for 30 min before cooling to RT. In-plane current over a voltage sweep from -10 to 10 mV was measured using probes with Pt-plated tungsten tips. Film resistance was calculated via linear regression of the current–voltage plots and used to calculate in-plane LSCF conductivity. Upon crystallization, a conductivity increase of approximately two orders of magnitude can be observed and hence serves as a suitable *in situ* probe of the structural evolution. The onset temperature for this change in conductivity is $\sim 440^\circ \text{ C}$ for both thin films, as observed in Fig. 3(b). A difference in the magnitude of conductivity between these films

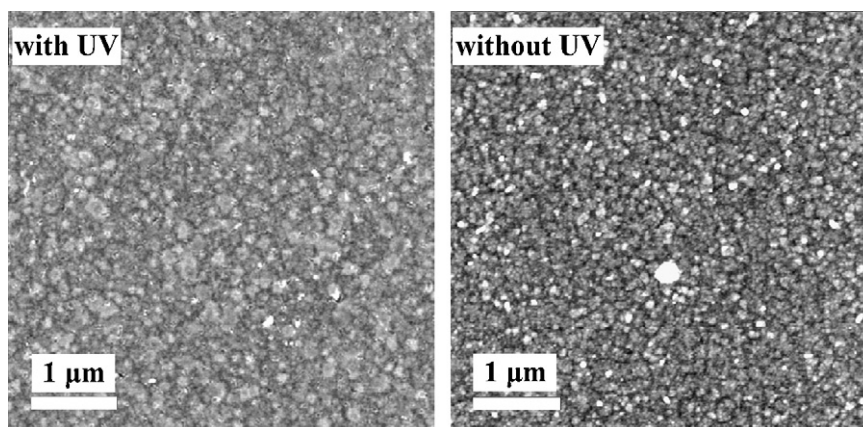


Fig. 2. AFM images of 60-nm-thick LSCF thin films annealed at 450 °C (a) with UV and (b) without UV irradiation.

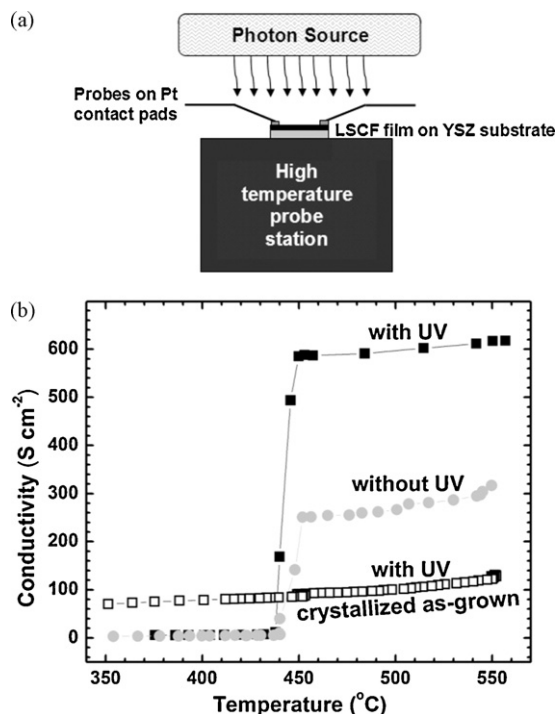


Fig. 3. (a) Schematic of experimental apparatus; (b) in-plane electrical conductivity vs. temperature for 60-nm-thick LSCF films annealed in air with UV (■) and without UV (●), as well as crystallized as-grown prior to measurement (□).

is observed at temperatures above the crystallization temperature up to 550 °C. The conductivity of the LSCF film annealed without UV was 248 S cm⁻¹ after 50 min at 450 °C. At the same temperature, after 40 min, the conductivity of the film annealed under UV irradiation was 588 S cm⁻¹. At 550 °C, conductivities were 320 and 618 S cm⁻¹ in films annealed without and with UV irradiation, respectively.

For comparison, a film deposited at 550 °C, which was crystalline as-grown and highly oxygen-deficient [13], was annealed up to 550 °C while being exposed to UV. The conductivity of the film crystallized in vacuum was higher than both amorphous films annealed in air up to the crystallization temperature. Past ~440 °C, the films annealed in air, both with and without UV annealing, exhibited higher conductivities up to 550 °C. This difference in conductivity suggests that conductivity in LSCF films is affected by the oxygen incorporation during crystallization. After the conductivity had stabilized at 450 °C, the photon source was turned off and the conductivity was re-measured. No appreciable difference in conductivity was observed. Accordingly, it is believed that UV radiation itself does not enhance the mechanism of charge conduction in LSCF; rather, it likely affects LSCF crystallization or stress through oxygen incorporation. Note that our recent studies show that conductivity is also related to grain size, cracks, and porosity [9,15].

Temporal changes in conductivity during crystallization at ~450 °C were investigated. Fig. 4 shows the evolution of conductivities for LSCF films annealed with and without UV. The maximum conductivity of the film annealed with UV is more than two times greater than the film annealed without UV, as seen in Fig. 2. Further, the rate at which the films approach their maximum conductivity is different. The film crystallized under UV approaches its maximum conductivity at 450 °C faster than the film crystallized without. Since electrical conductivity is related to the degree of crystallization, the data in Fig. 4 can be fitted similar to the Avrami exponent [22,23]: $\alpha = 1 - \exp(-(k(t - t_0)^n))$, where α is the fraction of crystallized material, k is a rate constant, n is the Avrami exponent,

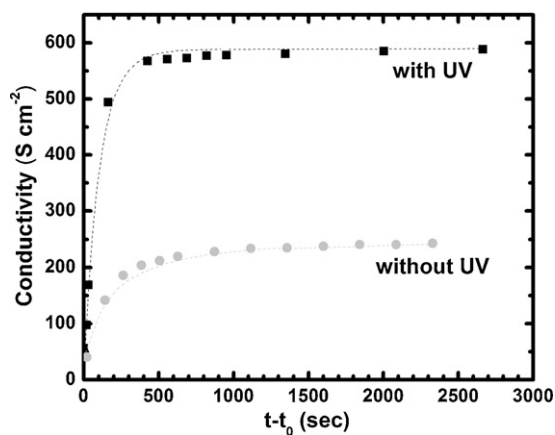


Fig. 4. Conductivity vs. time during crystallization of 60-nm-thick LSCF films at ~450 °C in air with UV (■) and without UV (●). Fitting results are represented by dash lines.

and t_0 is a time constant. The fitting results are shown in dash lines in Fig. 4. $n = 0.93$ is obtained for the case of annealing under UV; while it is $n = 0.62$ otherwise. This suggests that the crystallization rate of LSCF thin films is influenced by oxygen incorporation enabled by UV photons. Conductivity of the UV-annealed LSCF film was measured upon cooling from 550 °C and the activation energy was ~0.20 eV, consistent with reports on microcrystalline LSCF [8] and our reports on nanostructured LSCF thin films [9]. The result indicates the primary mechanisms involved in charge transport are essentially identical in these various cases.

4. Conclusion

We have demonstrated that UV assisted crystallization of RF-sputtered 60-nm-thick La_{0.6}Sr_{0.4}Co_{0.8}Fe_{0.2}O_{3- δ} thin films leads to superior electrical conductivity and enhanced crystallization kinetics. The sputtered LSCF films were observed to crystallize at ~440 °C. The difference in lattice parameter observed in films annealed under UV irradiation likely indicates increased oxygen concentration in LSCF films due to the presence of atomic oxygen and ozone during crystallization. The results indicate that photon-assisted processing could be a promising route for synthesis of nanostructured oxide cathodes.

Acknowledgement

We thank NNIN REU program and SiEnergy Systems for financial support.

References

- [1] B.C.H. Steele, A. Heinzel, *Nature* 414 (2001) 345–352.
- [2] J.W. Fergus, *JOM* 59 (December) (2007) 56–62.
- [3] N.Q. Minh, *Solid State Ionics* 174 (2004) 271–277.
- [4] S.M. Haile, *Acta Mater.* 51 (2003) 5981–6000.
- [5] S.J. Litzelman, J.L. Hertz, W. Jung, H.L. Tuller, *Fuel Cells* 5 (2008) 294–302.
- [6] J. Fleig, *Annu. Rev. Mater. Res.* 33 (2003) 361–382.
- [7] R. O'Hayre, S.W. Cha, W. Colella, F.B. Prinz, *Fuel Cell Fundamentals*, John Wiley & Sons, New York, USA, 2005.
- [8] L.-W. Tai, M.M. Nasrallah, H.U. Anderson, D.M. Sparlin, S.R. Sehlin, *Solid State Ionics* 76 (1995) 259–271.
- [9] B.-K. Lai, A.C. Johnson, H. Xiong, S. Ramanathan, *J. Power Sources* 186 (2009) 115–122.
- [10] F.S. Baumann, J. Fleig, G. Cristiani, B. Stuhlhofer, H.-U. Habermeier, J. Maier, *J. Electrochem. Soc.* 154 (2007) B931–B941.
- [11] S.B. Adler, J.A. Lane, B.C.H. Steele, *J. Electrochem. Soc.* 143 (1996) 3554–3564.
- [12] M. Prestat, J.-F. Koenig, L.J. Gauckler, *J. Electroceram.* 18 (2007) 111–120.
- [13] A.C. Johnson, B.-K. Lai, H. Xiong, S. Ramanathan, *J. Power Sources* 186 (2009) 252–260.

- [14] H. Xiong, B.-K. Lai, A.C. Johnson, S. Ramanathan, J. Power Sources 193 (2009) 589–592.
- [15] B.-K. Lai, H. Xiong, M. Tsuchiya, A.C. Johnson, S. Ramanathan, Fuel Cells 6 (2009) 699–710.
- [16] S. Ramanathan, D. Chi, P.C. McIntyre, C.J. Wetteland, J.R. Tesmer, J. Electrochem. Soc. 150 (2003) F110–F115.
- [17] A. Podpirka, M.W. Cole, S. Ramanathan, Appl. Phys. Lett. 92 (2008) 212906.
- [18] M. Tsuchiya, S. Ramanathan, Appl. Phys. Lett. 91 (2007) 253104.
- [19] M. Tsuchiya, S.K.R.S. Sankaranarayanan, S. Ramanathan, Prog. Mater. Sci. 54 (2009) 981–1057.
- [20] L. Fritzsche, H.J. Köhler, F. Thrum, G. Wende, H.G. Meyer, Physica C 296 (1998) 319–324.
- [21] P. Rottlander, H. Kohlstedt, P. Grunberg, E. Girgis, J. Appl. Phys. 87 (2000) 6067–6069.
- [22] R.W. Balluffi, S.M. Allen, W.C. Carter, Kinetics of Materials, John Wiley & Sons, Hoboken, NJ, 2005.
- [23] R. Luck, K. Lu, W. Frantz, Scripta Metall. Mater. 28 (1993) 1071–1075.